NASA TM X-263

N63-14965

C OdE -1

TECHNICAL MEMORANDUM
X-263

AN EXPERIMENTAL INVESTIGATION OF ABLATING MATERIALS

AT LOW AND HIGH ENTHALPY POTENTIALS

By Bernard Rashis and Thomas E. Walton, Jr.

Langley Research Center
Langley Field, Va.

401 _ _ 554188 _ _ _ _

NATIONAL AERONAUTICS AND SPACE ADMINISTRATION

WASHINGTON   March 1960

NATIONAL AERONAUTICS AND SPACE ADMINISTRATION

TECHNICAL MEMORANDUM X-263

AN EXPERIMENTAL INVESTIGATION OF ABLATING MATERIALS

AT LOW AND HIGH ENTHALPY POTENTIALS*

By Bernard Rashis and Thomas E. Walton, Jr.

SUMMARY

14765

The ablation performance characteristics of a number of materials were derived from tests conducted in a Mach number 2.0 ethylene-heated high-temperature air jet having a maximum stagnation enthalpy potential of approximately 1,200 Btu/lb. The tests were conducted with 6-inch-diameter blunt nose shapes. The surface of most of the materials after testing was generally smooth and the unablated portions of the specimens were in appearance the same as before testing. In all cases, the back or inside surface of the specimens exhibited no evidence of heating.

An evaluation of the enthalpy potential effect was obtained by comparison of the present data with previous tests conducted, on the 6-inch-diameter blunt-face configuration, in a subsonic arc-heated air jet. The stagnation enthalpy potential of this facility was approximately 7,000 Btu/lb. For Teflon, the effective heat of ablation increased from approximately 1,250 Btu/lb to 3,900 Btu/lb when the stagnation enthalpy potential was increased from 800 Btu/lb to 7,000 Btu/lb.

INTRODUCTION

In previous investigations (refs. 1 and 2) of ablating materials, the test conditions were limited to short-time duration, high aerodynamic heat flux, and low stagnation enthalpies. For these conditions, the derived results indicated that an ablation shield was capable of providing adequate thermal protection for the inner structure. However, for some applications, such as manned reentry vehicles, the trajectories have long time duration, low aerodynamic heat flux, and high stagnation enthalpy.

---

*
Title, Unclassified.

Although theory (ref. 3) indicates that the effectiveness of the ablating material increases with stagnation enthalpy, low heat flux and long time could conceivably cause deterioration of the material. Since deterioration and stagnation enthalpy effects could be critical, experimental evaluations of a number of selected materials of the same configuration were undertaken in two ground facilities which had widely different stagnation enthalpies. The test conditions varied with regard to test time duration and heat-flux range, depending on the particular limitations of the facility used.

The tests were made in the ethylene-heated high-temperature air jet of the NASA Wallops Station, which has a Mach number of 2.0 and a maximum stagnation enthalpy potential of approximately 1,200 Btu/lb, and in a subsonic arc-heated air jet at the Chicago Midway Laboratories (CML), which has a stagnation enthalpy potential of approximately 7,000 Btu/lb. The operating characteristics of these two facilities are given in table I.

The CML tests were part of a study conducted under the joint cognizance of the Wright Air Development Center, the Air Force Ballistic Missile Division, and the National Aeronautics and Space Administration. The CML test results are given in reference 4.

This paper evaluates the ablation performance characteristics of the various materials as derived from both series of tests. The tests in both facilities were conducted at essentially the same aerodynamic heat flux, approximately 100 Btu/(sq ft)(sec).

SYMBOLS

h heat-transfer coefficient, Btu/(sq ft)(sec)(^{O}F)

h_{eff} effective heat of ablation, Btu/lb

ΔH enthalpy potential difference across boundary layer, Btu/lb

$\dot{m}$ ablation rate, lb/(sq ft)(sec)

p surface pressure, lb/sq ft

p_{t2} stagnation pressure behind normal shock, lb/sq ft

q aerodynamic heat flux, Btu/(sq ft)(sec)

r nose radius, ft

r_c	radius of curvature of nose, ft
s	distance along surface from stagnation point, ft
t	time, sec
T	temperature, $^\circ F$
x	recession distance measured normal to nose surface, ft
ϵ	emissivity
ρ	specific weight, lb/cu ft
σ	Stefan-Boltzmann constant, 0.481×10^{-12} Btu/(sq ft)(sec)($^\circ R$)

Subscripts:

eq	equilibrium values
f	final values
i	initial values
o	stagnation point values
rad	radiation
w	wall values

<div align="center">TEST FACILITIES AND PROCEDURE</div>

The NASA tests were conducted in the ethylene-heated high-temperature air jet of the NASA Wallops Station. This facility is capable of producing a hot jet having a free-stream Mach number of 2.0 and stagnation temperatures to 3,500° F. The jet exhausts at sea-level pressure and has a maximum stagnation enthalpy potential of approximately 1,200 Btu/lb. A detailed description of the physical characteristics of this facility is given in reference 5.

The models were mounted on a side-injection-type sting (fig. 1) and were inserted into the jet stream only after steady flow conditions were established. A timer which was synchronized with the sting was visually recorded along with the models for all the tests by high-speed motion-picture cameras. These cameras were a 16-mm camera using color film and

<div align="center">CONFIDENTIAL</div>

operating at 128 frames per second and located directly above the model, a 35-mm camera using black-and-white film and operating at 10 frames per second and located directly to the side, and a surface-temperature measuring camera operating at 1 frame every 2 seconds and located slightly upstream and to the side.

The CML tests were conducted in a subsonic arc-heated air jet which has a stagnation enthalpy potential of approximately 7,000 Btu/lb. The details of this facility and the operation characteristics of the jet are given in reference 6. The test procedures for the CML tests are given in reference 4. The operating characteristics of both test facilities are given in table I.

A photographic technique (ref. 7) was employed to obtain measurements of the surface temperature for the tests with the ablating shields. The basic principle of the photographic technique is relatively straightforward. If a photograph is taken of an object which is luminous, the resulting negative will be darkest in the regions of highest temperatures and lightest in the regions of low temperatures. Since the measured temperature is proportional to the logarithmic variation of film density, measurements of the film density provide the information for obtaining surface temperatures. The technique used in these tests is feasible whenever the object has been heated to a temperature (approximately 1,400° F) sufficiently high so that the surface is luminous and if the surface can be considered a gray-body radiator of known emissivity.

MODELS AND INSTRUMENTATION

Figure 2 shows the details and the locations of the thermocouples and pressure orifices of the calorimeter model. Figure 3 shows the details of the ablation shield protected models. The basic configuration was a blunt nose shape having a ratio $r/r_c = 1/3$ and a 15° boattailed afterbody.

The ablation shields of configuration A were bonded by using epoxy resins to the Inconel shell faces. For the Teflon material, this type of bonding was not satisfactory and screws made of Teflon were used to fasten the shield to the shell face. The ablation shields of configuration B were fastened to the shells with steel bolts that were located well within the nonablating regions of the shields. The shields were insulated from the shells by 1/16-inch-thick glass wool.

The materials studied are listed in table II. With the exception of the mixture of 75-percent ammonium chloride and 25-percent silicone

rubber resin (Dow-Corning S6015A), all of the shields were constructed from commercially obtained materials.

The calorimeter model (fig. 2) was instrumented with six thermocouples spot-welded to the inside surface of the shell face. Three pressure orifices were located on the face and three along the afterbody.

The models of configuration A were instrumented with five thermocouples spot-welded to the inside surface of the shell faces. The models of configuration B had a thermocouple cemented to the back surface and located on the center line.

DATA REDUCTION

For all the tests the recession distances x were determined from enlargements of the motion-picture film. The values obtained in this manner were checked by means of the jig shown in figure 4. The jig was designed to hold a dial gage at various locations over the nose-shape surface. The ablation rates $\dot{m}$ determined by this method are local values and are computed from

$$\dot{m} = \rho \, \frac{x_i - x_f}{t_f - t_i}$$

where ρ is the specific weight of the ablation-shield material.

The heat inputs to the ablating nose shapes were computed from

$$q_o = h_o\left(T_o - T_w\right) - \sigma \epsilon T_w^4$$

the last term being the correction due to radiation. The value of h_o was determined from calorimeter tests made with the model shown in figure 2. The calculated radiation term for all the calorimeter tests was negligible compared with the quantity $h_o\left(T_o - T_w\right)$. The heat-transfer variation h/h_o across the nose shape is shown in figure 5. The stagnation-point value h_o of 0.055 Btu/(sq ft)(sec)($^\circ$F) was assumed constant for all tests. Although not required for these tests, the pressure variation along the configuration was measured. The results are shown in figure 6. For comparison purposes the variations for a flat face and a hemisphere (ref. 8) are also shown.

RESULTS AND DISCUSSION

Visual Observations of Specimens

Examination of the color motion pictures and the models tested in both the ethylene- and arc-heated jets indicated that all the Teflon models acted in essentially the same manner. The Teflon surface was slick throughout the tests; there was no visible sign of flaming or melting during the tests and after testing the Teflon showed no sign of discoloration. For one of the tests conducted in the ethylene jet, the motion-picture camera was kept focused on a Teflon model for a period of time after the test. Considerable distortion of the Teflon was observed during this cooling period, but during the test no distortion occurred. The reverse of this was observed with one of the models of reference 1. The Teflon swelled and distorted during the heating phase and upon removal from the jet the swelling and distortion was rapidly alleviated.

Figure 7 shows one of the Teflon models after being exposed to a stagnation temperature of 3,300° F for 20 seconds. The weight loss was 0.4370 pound. This value was corrected for the weight loss caused by irregular heating around holes that had been drilled into the material. These holes are seen in figure 7. The holes were drilled for thermocouples; however, no temperature data were obtained from these thermocouples and, hence, temperature data are not presented.

The nylon model, which was tested only in the ethylene jet, showed no sign of flaming or melting during the tests. No discoloration of the surface occurred during or after the tests. There was no visible evidence of distortion or swelling at any time during the tests or after the tests. Figure 8 shows one of the nylon models after being exposed to a stagnation temperature of 1,750° F for 20 seconds. The nylon surface ablated very smoothly and the weight loss during the test was 0.2827 pound. No discoloration of the nylon was noted during or after the test.

The Plexiglas model acted essentially the same in both the ethylene- and arc-heated facilities. There were no signs of vapor, flaming, or melting. The surface after testing was very smooth. Figure 9 shows the Plexiglas 55 specimen after 19.56 seconds exposure to a stagnation temperature of 3,300° F. The weight loss was 0.5280 pound. This value was corrected for the weight loss by breaking off of material. This breaking off of material occurred when the specimen was being removed from the support sting. The discoloration shown in figure 9 was caused from tight contact with the insulating material.

The NASA samples, which were tested in the ethylene jet, did not show any signs of flaming or melting. There were signs of vaporization and occasional flaking of the material occurred. During the tests this

material swelled but upon removal from the jet the swelling immediately began to go down. The surface of this material was relatively rough after testing.

All the reinforced plastic materials acted in essentially the same manner. The materials glowed very brightly during the tests and upon removal from the jet, most of the materials showed some flaming.

Figure 10 shows the Formica YN-25 specimen after being exposed to a stagnation temperature of 3,300° F for 30 seconds. The weight loss was 0.3010 pound. Although the surface was blackened, indicating some charring, there was no significant thickness of charred layer on the surface of the specimen.

Figure 11 shows the Formica LN-42 specimen after being exposed to a stagnation temperature of 3,300° F for 30 seconds. The weight loss was 0.436 pound. Although the surface shows indentations and does not appear smooth, as for example the nylon-phenolic material, the depths of the indentations are very small and the surface is actually relatively regular. Although the surface was blackened indicating charring, there was no significant thickness of a charred layer on the surface of the specimen.

The Formica CH-41 specimen was tested for 28.5 seconds at a stagnation temperature of 3,300° F but no data on weight losses were obtained for this specimen because destruction of the model occurred during the test.

Figure 12 shows the Raybestos 42RPD specimen after 40 seconds exposure to a stagnation temperature of 3,300° F. The weight loss was 0.160 pound. The thickness of the char layer at the stagnation point was approximately 0.07 inch. The surface of this specimen was very rough, having an appearance much like a house roof with some of the shingles missing. However, the material underneath the char layer was essentially unaffected.

Figure 13 shows the Cincinnati Testing Laboratory material after exposure to a stagnation temperature of 3,300° F for 30 seconds. The weight loss was 0.230 pound. The thickness of the char layer at the stagnation point was approximately 0.10 inch. The surface of the specimen was very hard and relatively smooth and underneath the char layer the material showed virtually no signs of being heated.

Figure 14 shows the Astrolite specimen after 20 seconds exposure to a stagnation temperature of 3,300° F. The weight loss was 0.0588 pound and thickness of the char at the stagnation point was approximately 0.10 inch. The surface was in excellent condition after the test; however, there was some separation of the Refrasil fibers underneath the char layer.

It should be noted that without exception, the surface appearance of the specimens tested in the ethlyene-heated air jet were practically the same as the surface appearance of the same materials when they were tested in a subsonic arc-heated air jet facility at CML.

Ablation Effectiveness of Nonreinforced Materials

The results obtained from the two facilities are shown in figure 15 where the stagnation-point ablation rate is plotted as a function of the stagnation temperature. The test results in the stagnation temperature range from 1,750° F to 3,300° F were obtained from the ethylene jet and the results for the stagnation temperature of 10,340° F were obtained from the CML arc-heated air jet. Note that, as indicated in table I, both series of tests were made at stagnation heat fluxes of approximately 100 Btu/(sq ft)(sec). The data shown in figure 15 along with the pertinent test conditions are summarized in table III. In determining the ablation rates, the recession distance was considered as the difference between the original material thickness and the uncharred or unaffected material thickness. (The recession distances listed in reference 4 were measured to the top of the char layer.) For the CML tests, the time duration was considered to be only that of the air-arc heating cycle since the initial preheating caused essentially no ablation.

Figure 16 shows the variation of the ablation rates and heat fluxes across the face of the nylon model. The correlation of the ablation rates with the heat flux values indicates that erosion effects for the nylon material were negligible. (For no erosion, $\dot{m}$ is proportional to q.)

Recession distances along the specimen surface were obtained from the 35-mm black-and-white film for all the models tested; however, only the nylon was free of surface irregularities, swelling, or distortion, which prevented accurate checking of the film data by means of the jig for the other materials tested. The ablation rate and heat flux variation across the face for most of the other materials was similar to that shown in figure 16 but the scatter of the individual point values was too large to allow any quantitative interpretation.

Defining the effective heat of ablation parameter h_{eff} as

$$h_{eff} = \frac{q}{\dot{m}}$$

the value at the stagnation point derived from the ethylene jet tests for the nylon is 934 Btu/lb. The enthalpy potential for this data point

was 252 Btu/lb. In deriving these values, the ablating surface tempera-
ture was assumed to be 800° F, or 200° F above the melting temperature
of nylon.

For the NASA sample (75-percent ammonium chloride and 25-percent
silicone rubber resin), the derived value of h_{eff} at the stagnation
point was 1,400 Btu/lb. The enthalpy potential was 505 Btu/lb. This
value was derived by using an ablating surface temperature of 635° F.
This is the value given for the sublimation temperature of ammonium
chloride in reference 9.

For the Teflon model, h_{eff} values were derived from tests in both
the ethylene- and arc-heated jets. The derived values were in agreement
with the theory of reference 3 with respect to improved effective heats
of ablation at higher enthalpy potentials. The derived values of h_{eff}
at the stagnation point increased from 1,250 Btu/lb to 3,900 Btu/lb when
the stagnation enthalpy was increased from 800 Btu/lb (ethylene jet) to
7,000 Btu/lb (arc jet). For Teflon, the calculated ablating surface
temperature increases with the ablation rate as shown in figure 17. The
values given in figure 17 were obtained from reference 10.

For the Plexiglas 55 model, the derived values of h_{eff} at the
stagnation point increased from 1,300 Btu/lb to 2,750 Btu/lb when the
stagnation enthalpy potential was increased from 1,030 Btu/lb to
7,000 Btu/lb. In deriving these values, the surface temperature was
assumed to be 500° F, or 200° F above the melting temperature.

The effective heats of ablation for Teflon, Plexiglas 55, nylon,
and ammonium chloride mixture (NASA sample) are shown in figure 18, as
a function of the enthalpy potential across the boundary layer, ΔH_0.
The equations of the lines connecting the Teflon and Plexiglas 55 test
results are as follows:

for Teflon

$$h_{eff_0} = 900 + 0.43 \; \Delta H_0$$

and for Plexiglas

$$h_{eff_0} = 1,075 + 0.235 \; \Delta H_0$$

Although the preceding expressions are derived from the results
of the present paper, the theory of reference 3 indicates that the varia-
tion of h_{eff} with enthalpy potential is approximately linear. Thus,
the preceding expressions are believed to be reasonably valid for the
enthalpy potential range covered by the tests.

Ablation Effectiveness of Reinforced Plastic Materials

All the reinforced plastics (fibrous reinforcements and resin binders) were tested in the ethlyene jet at a stagnation temperature of 3,300° F. For this test condition, the calculated radiation equilibrium surface temperature for an emissivity of 0.7 (value assumed for all the reinforced plastics) was 2,700° F. The measured surface-temperature values, as derived from the photographic technique, however, ranged from 3,000° F to 3,200° F. It appears likely, therefore, that exothermic reactions occurred between the resin binders and the jet exhaust products.

Figure 19 shows the temperature histories for the Formica YN-25 model. The temperature curves for the other two Formica models were essentially the same. Although the surface temperatures were very high, the inside surface temperatures of the materials remained at ambient level throughout the durations of the tests.

The other reinforced plastic materials which were tested were Raybestos 42RPD (asbestos, phenolic resin), Cincinnati Testing Laboratory material (Fiberglas, phenolic resin), Astrolite (Refrasil, phenolic resin). For the Raybestos and Astrolite models there was no measureable recession of the exposed surfaces. This was also true for the Cincinnati Testing Laboratory material except at the outer edges of the nose shape where a very slight recession was measured. These three specimens had measureable weight losses and examination indicated that, to a depth of approximately 0.1 inch, the resin binders had boiled or vaporized out of the material.

Since the reinforcement materials remained intact, they were able to continue absorbing heat. The exposed surface temperatures for these three materials kept increasing during the test time durations, the trend being essentially similar to that for a nonablating material. This effect is shown in figure 20 which shows the temperature histories for the Raybestos 42RPD model. (The temperature-histories for the other two materials were essentially the same.) It should be noted that, although steady-state ablation of the reinforcement materials did not occur for these tests, the back or inside surfaces of the test specimens remained essentially at ambient temperature.

The results indicate that, for these test conditions, mass-transfer cooling was achieved just from the resin binders. Under test conditions where the reinforcement material would also ablate, the performance of these materials would depend on the ratio of the specific heats of both the binder and the reinforcement vapors. Improved values would be obtained if the specific heat of the reinforcement material vapor was greater than that of the binder.

Because of uncertainties in the surface temperatures and in the magnitude of the exothermic reactions, a quantitative comparison of the

effective heats of ablation for the reinforced plastic materials was not made. However, a qualitative comparison is given in figure 21. Since h_{eff} is proportional to $1/\dot{m}$, an indication of the performance characteristics is obtained by plotting $1/\dot{m}$ against the estimated stagnation enthalpy potential ΔH_O. Since within the separate facilities, the jet conditions were maintained constant for each set of materials, figure 21 indicates the ranking of the materials under two separate sets of jet conditions. The values for Plexiglas 55 for which h_{eff} was determined have been included for comparison purposes.

SUMMARY OF RESULTS

The ablation performance characteristics of a number of materials were derived from tests conducted in both ethylene and arc-heated air jets. For the tests in the ethylene-heated jet, the maximum stagnation enthalpy potential was 1,200 Btu/lb, whereas for the tests in the arc-heated jet the stagnation enthalpy potential was 7,000 Btu/lb. The tests in both facilities were conducted of essentially the same stagnation aerodynamic heat fluxes, approximately 100 Btu/(sq ft)(sec). The following results were obtained:

1. The surface of most of the materials after testing was generally smooth and the unablated portions of the materials (underneath the char layer) showed no visible signs of deterioration. In all cases, the back or inside surfaces of the specimens exhibited no signs of heating.

2. All of the materials had lower values of mass loss in the arc-heated jet indicating that the effectiveness of ablating materials improves with increasing stagnation enthalpy. For example, the effective heat of ablation for Teflon increased from 1,250 Btu/lb to 3,900 Btu/lb when the stagnation enthalpy potential was increased from 800 Btu/lb to 7,000 Btu/lb.

Langley Research Center,
    National Aeronautics and Space Administration,
        Langley Field, Va., December 8, 1959.

CONFIDENTIAL

REFERENCES

1. Rashis, Bernard, Witte, William G., and Hopko, Russell N.: Qualitative Measurements of the Effective Heats of Ablation of Several Materials in Supersonic Air Jets of Stagnation Temperatures Up to 11,000° F. NACA RM L58E22, 1958.

2. Bond, Aleck C., Rashis, Bernard, and Levin, L. Ross: Experimental Ablation Cooling. NACA RM L58E15a, 1958.

3. Lees, Lester: Similarity Parameters for Surface Melting of a Blunt-Nosed Body in a High Velocity Gas Stream. Rep. No. GM-TM-184 (Contract No. AF 18(600)-1190), Guided Missile Res. Div., The Ramo-Wooldridge Corp., July 29, 1957.

4. Anon.: Thermal Protection of Structural Propulsion, and Temperature Sensitive Materials for Hypersonic and Space Flight. CML-DR-M152-2 (Contract No. AF 33(616)-6006), Chicago Midway Labs., October 21, 1958.

5. English, Roland D., Spinak, Abraham, and Helton, Eldred H.: Physical Characteristics and Test Conditions of an Ethylene-Heated High-Temperature Jet. NACA TN 4182, 1958.

6. Bonin, John H., Price, Channon F., and Taylor, Donald E.: Determination of Factors Governing Selection and Application of Materials for Ablation Cooling of Hypervelocity Vehicles. WADC Tech. Rep. 59-87, Pt. I, U.S. Air Force, July 1959.

7. Siviter, James H., Jr.: Photographic Technique of Surface Temperature Measurement. Presented at Third Pacific Area National Meeting (San Francisco, Calif.), ASTM, Oct. 11-16, 1959.

8. Stoney, William E., Jr., and Markley, J. Thomas: Heat Transfer and Pressure Measurements on Flat-Faced Cylinders at Mach Number 2. NACA TN 4300, 1958.

9. Hodgman, Charles D., ed.: Handbook of Chemistry and Physics. Thirty-sixth ed., Chemical Rubber Publ. Co., 1954-1955.

10. Steg, Leo: Materials For Re-Entry Heat Protection of Satellites. [Preprint] 836-59, presented at the Am. Rocket Soc. Semi-Annual Meeting (San Diego, Calif.), June 1959.

DECLASSIFIED

TABLE I.- JET CHARACTERISTICS

Characteristic	Ethylene-heated jet (ref. 5)	Arc-heated jet (ref. 6)
Mach number	2.0	0.2
Stagnation temperature, $^\circ$F . . .	3,300	10,340
Stagnation enthalpy potential, Btu/lb	1,200	6,000 to 7,000
Dynamic pressure, lb/sq ft . . .	6,000	50
Heat source	Ethylene combustion	Electric arc
Stagnation heat flux, Btu/(sq ft)(sec)	100 to 125	110
Test time duration, sec	20 to 40	124

TABLE II.- PHYSICAL CHARACTERISTICS OF MATERIALS TESTED

Material	Resin	Fiber	Fiber orientation (a)	Specific weight, lb/cu ft
Formica YN-25	Phenolic	Nylon fabric	Parallel	76
Formica LN-42	Phenolic	Cotton fabric	Parallel	87
Formica CH-41	Melamine	Cotton fabric	Parallel	93
Plexiglas 55	Methyl Methacrylate	-------------	----------	72
Astrolite	Phenolic	Refrasil	Random (chopped fabric)	106
Raybestos 42RPD	Phenolic	Asbestos	----------	118
Cincinnati Testing Lab.	Phenolic	Glass fabric	Random (chopped fabric)	126
Teflon	Teflon	-------------	----------	132
NASA sample	25-percent silicone gum rubber	75-percent ammonium chloride	----------	86
Nylon	Nylon	-------------	----------	70

[a]With respect to back surface of specimens.

TABLE III.- SUMMARY OF TEST RESULTS

Material	NASA tests, ethylene-heated jet		CML tests, arc-heated jet	
	T_O	$\dot{m}$	T_O	$\dot{m}$
Formica YN-25	3,300	0.02585	10,340	0.0174
Formica LN-42	3,300	.03490	10,340	.0220
Formica CH-41	3,300	.06225	10,340	.0294
Plexiglas 55	3,300	.0829	10,340	.0406
Astrolite	3,300	.0442	10,340	.0261
Raybestos 42RPD	3,300	.01720	10,340	.01405
Cincinnati Testing Lab.	3,300	.02735	10,340	.01818
Teflon	3,300	.06725	10,340	.02810
NASA sample	2,500	.08140	------	-------
Nylon	1,750	.05472	------	-------
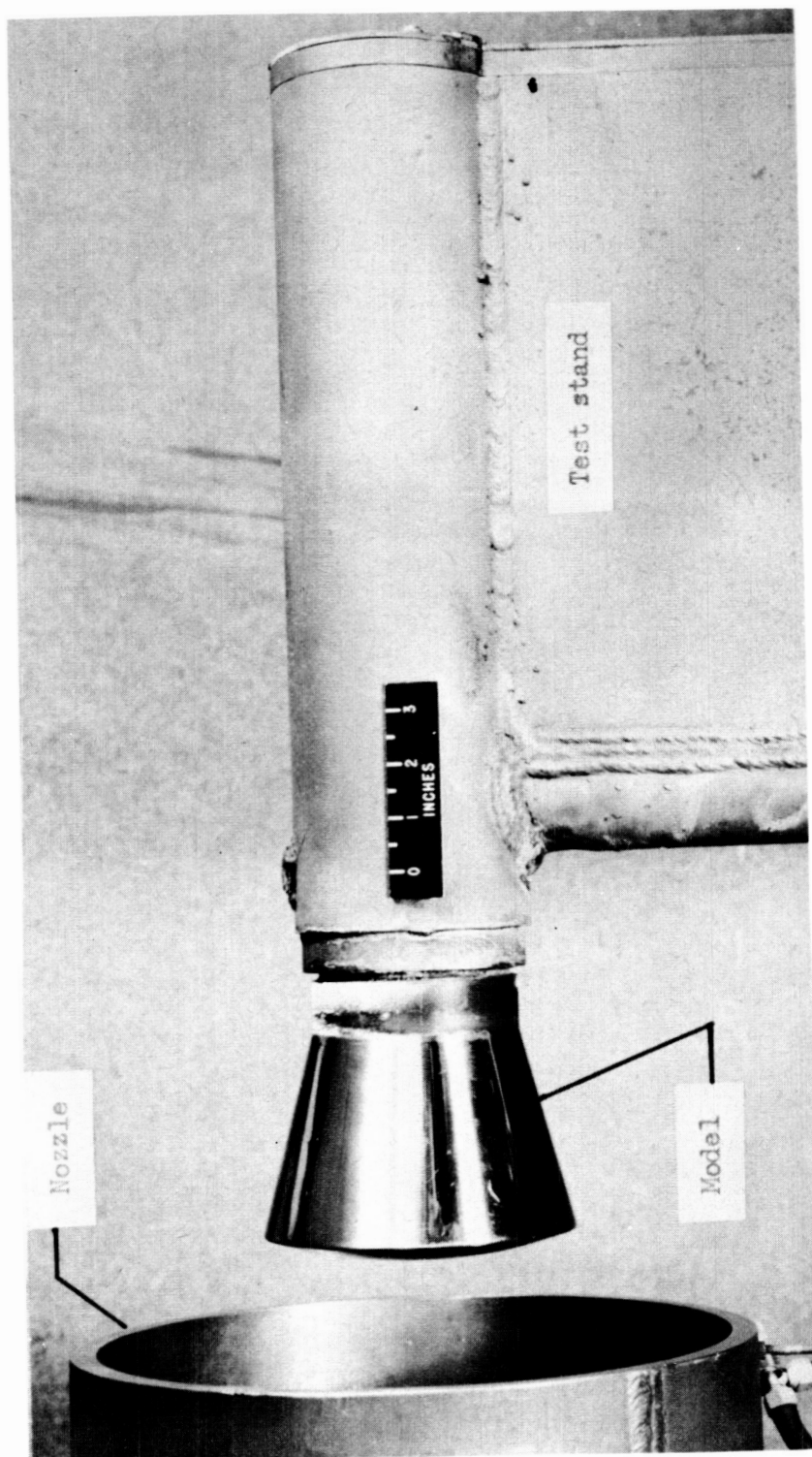
Figure 1.- Calorimeter model and test stand.   L-58-3483.1

Figure 2.- Inconel calorimeter model. All dimensions are in inches.

(a) Configuration A.

Thermocouple Location, s, in.	
1	0.5
2	1.0
3	1.5
4	2.0
5	2.5
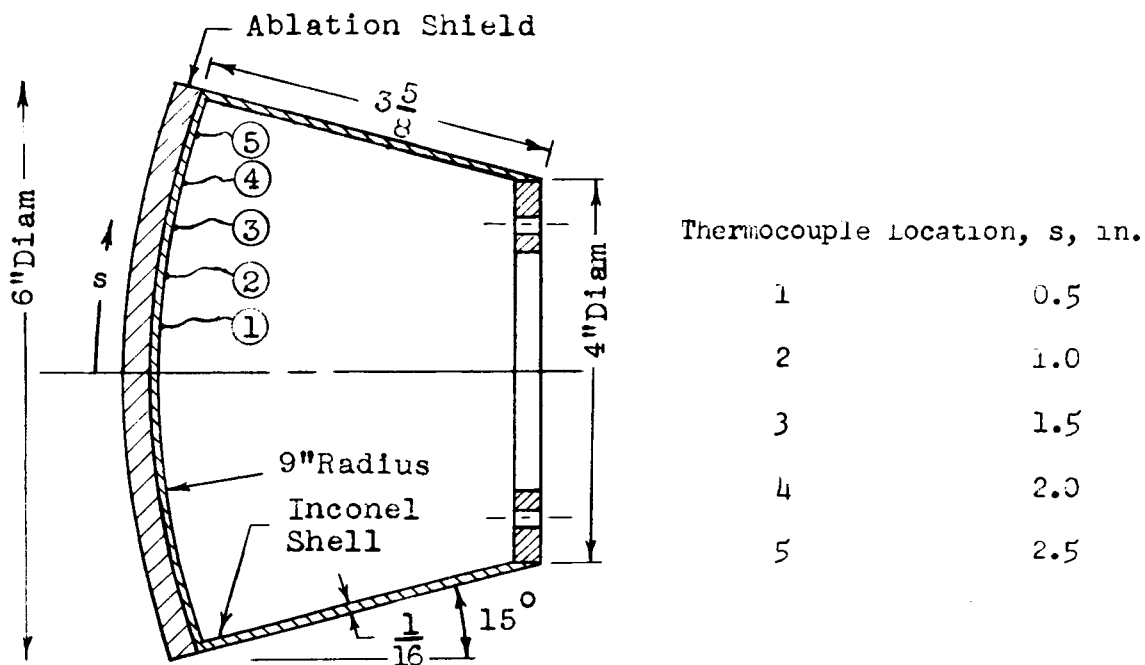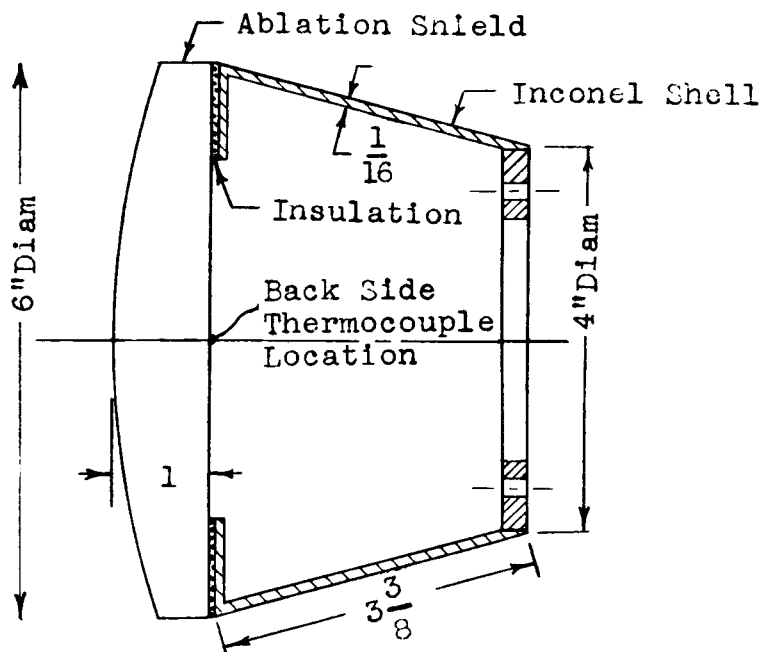
(b) Configuration B.

Figure 3.- Ablation model configurations and thermocouple locations.
All dimensions are in inches.
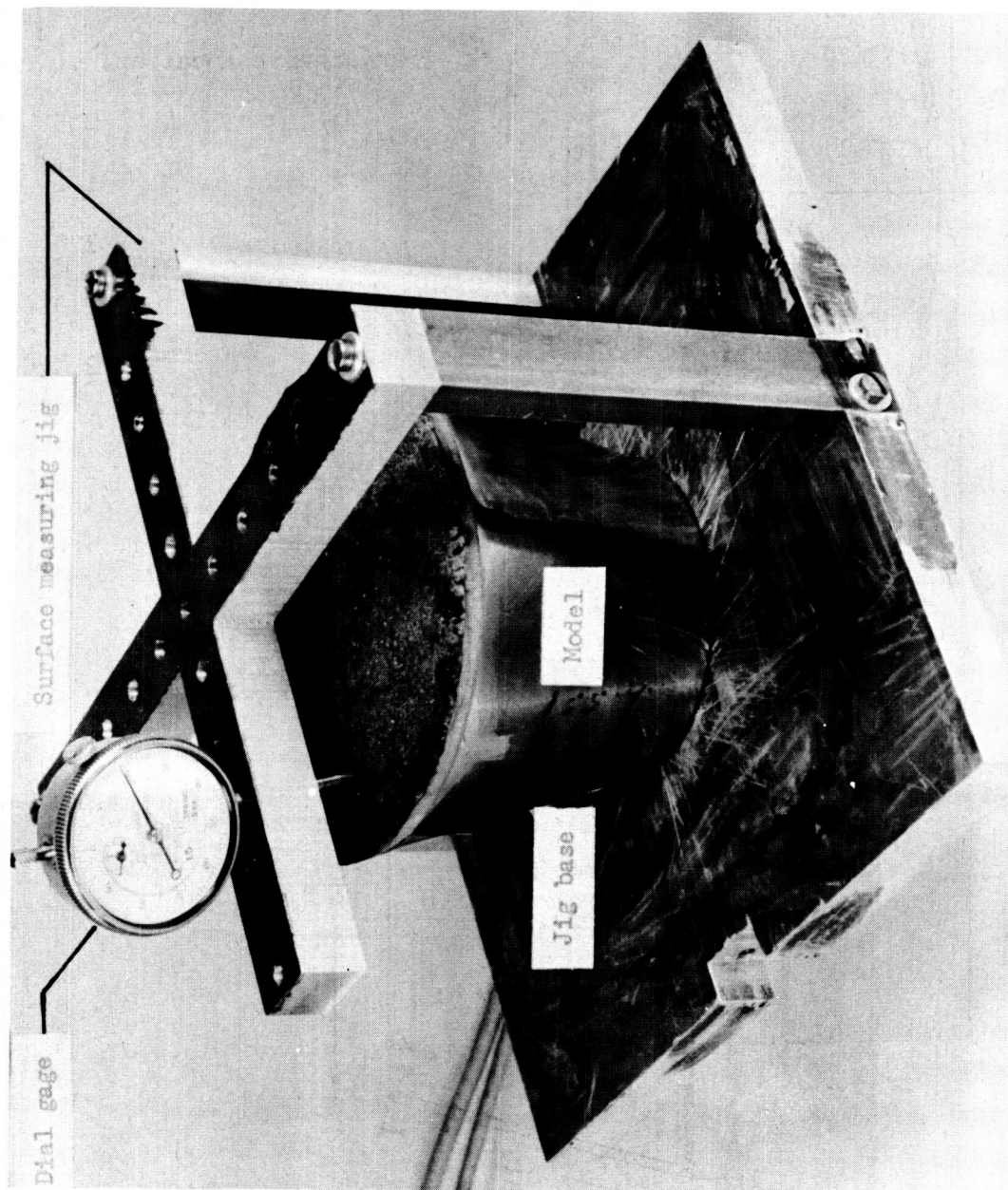
Figure 4.- Ablation model and surface measuring jig.

L-58-4252.1
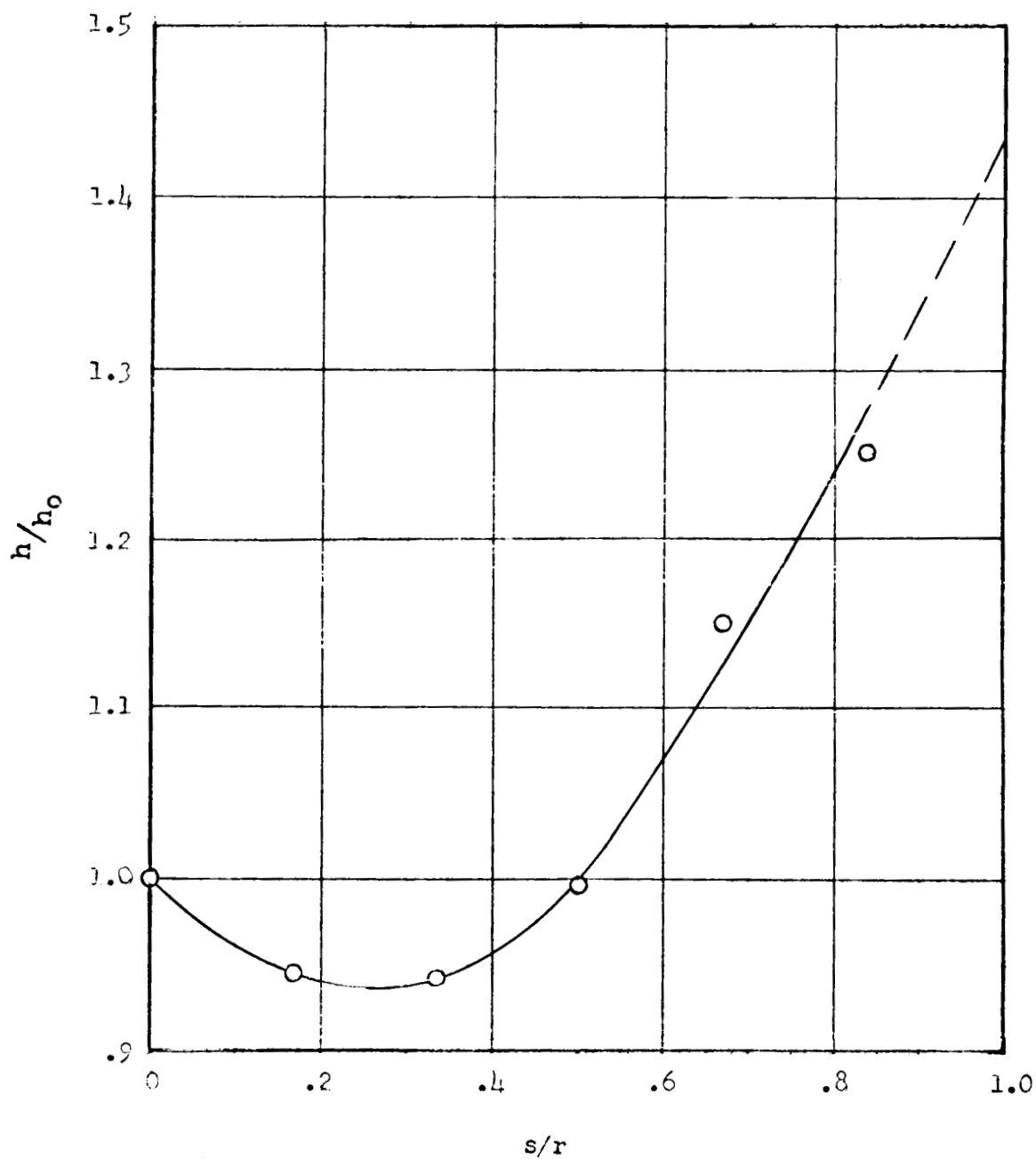
Figure 5.- Variation of heat-transfer coefficient across noseshape. $h_o = 0.055$ Btu/(sq ft)(sec)(^{o}F); $T_o = 1,016^o$ to $1,830^o$ F.
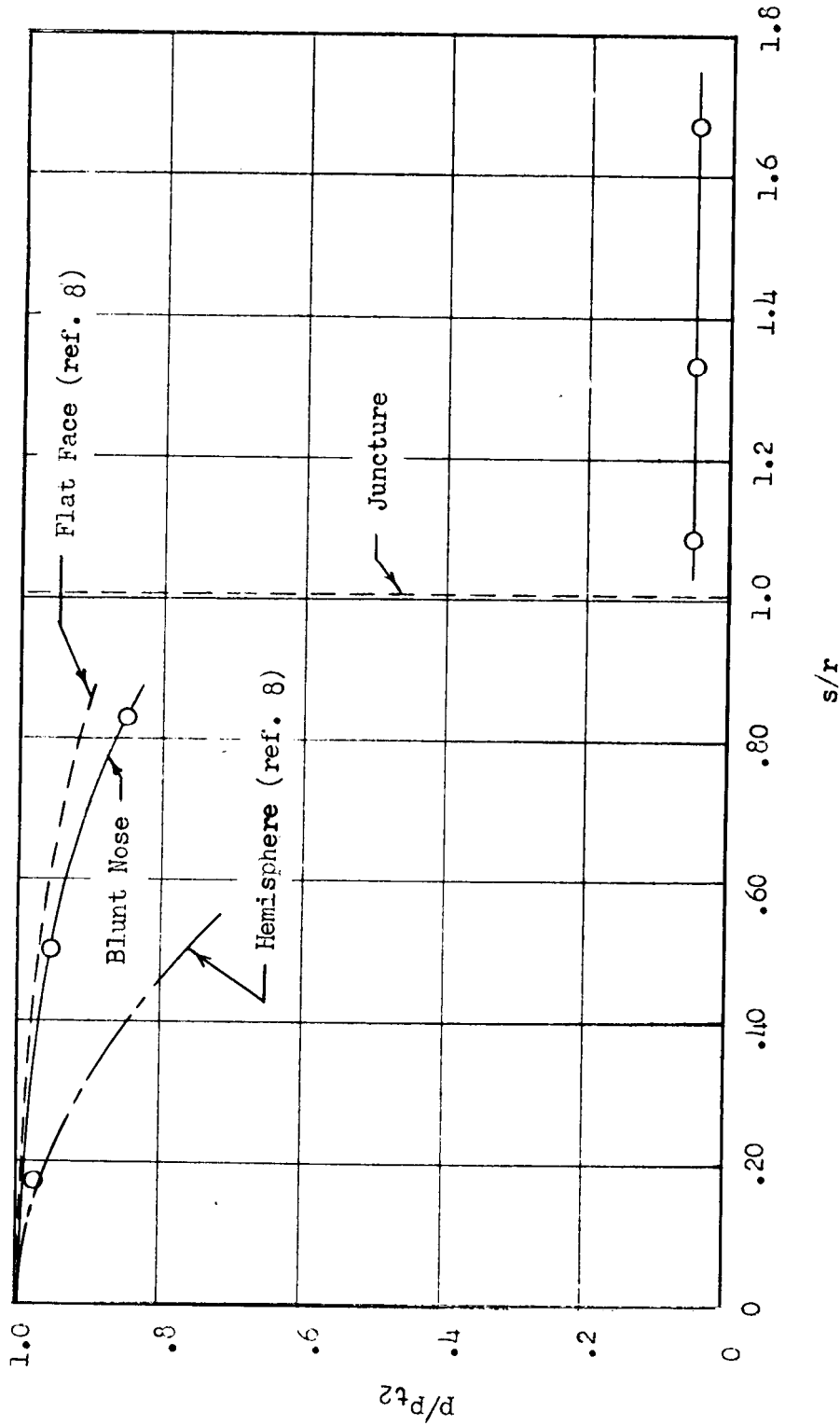
Figure 6.- Pressure variation across noseshape and afterbody.

| ,0 | 1 | ,2 |
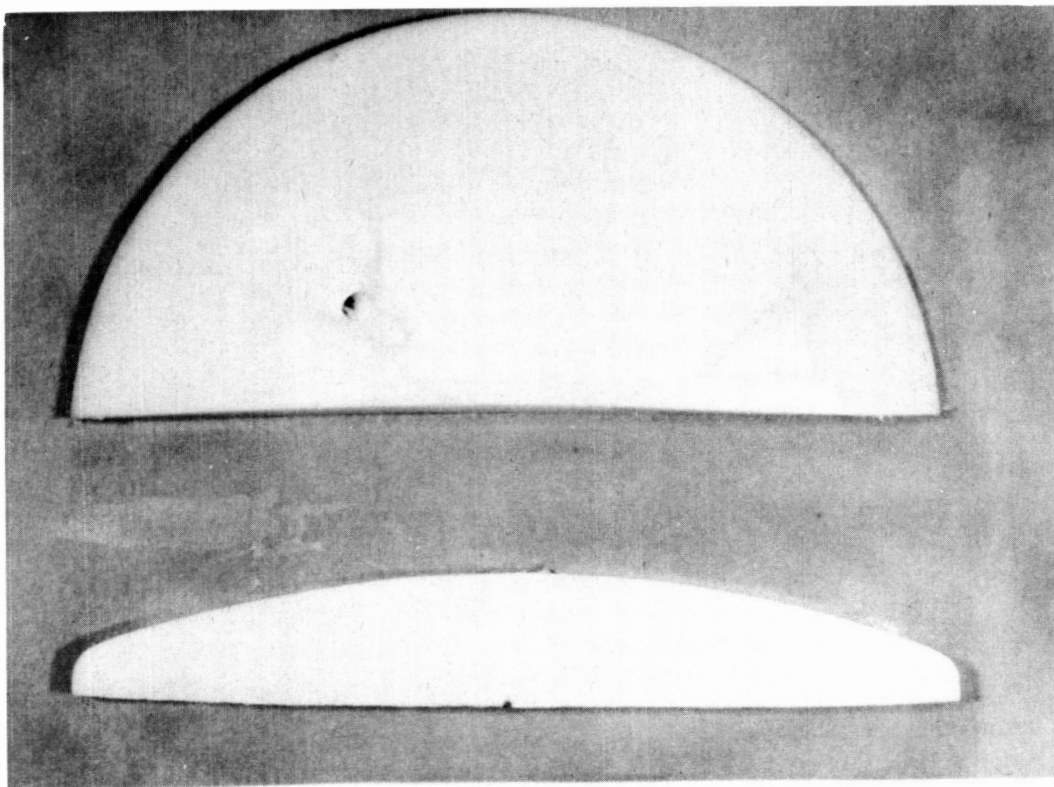
L-58-861a

Stagnation temperature, °F 3,300
Test time, sec 19.80
Weight loss, lb 0.4370

Figure 7.- Surface appearance of Teflon specimen after ablation.

```
                                                          L-59-732
Stagnation temperature, °F . . . . . . . . . . . .    1,750
Test time, sec . . . . . . . . . . . . . . . . . .    20.05
Weight loss, lb  . . . . . . . . . . . . . . . . .    0.2827
```

Figure 8.- Surface appearance of nylon specimen after ablation.

Stagnation temperature, °F 3,300
Test time, sec 19.56
Weight loss, lb 0.5280

Figure 9.- Surface appearance of Plexiglas 55 specimen after ablation.

L-58-856a

Stagnation temperature, °F   3,300
Test time, sec 30.00
Weight loss, lb 0.3010

Figure 10.- Surface appearance of Formica YN-25 specimen after ablation.

CONFIDENTIAL
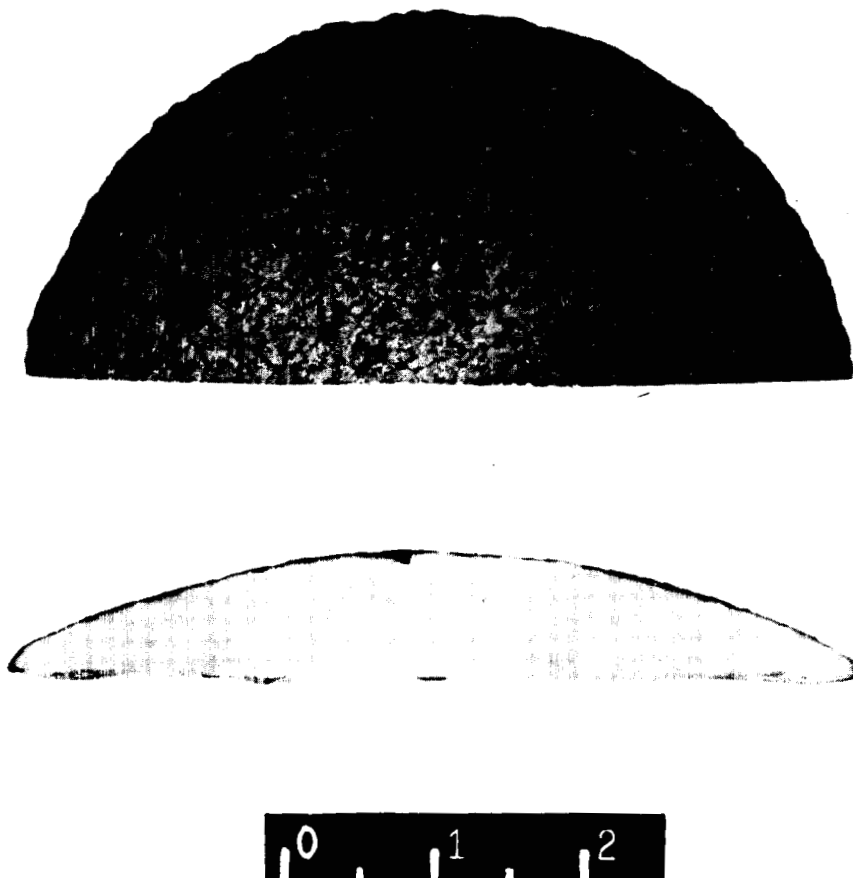
L-58-857a

Stagnation temperature, °F   3,300
Test time, sec 30.00
Weight loss, lb 0.436

Figure 11.- Surface appearance of Formica LN-42 specimen after ablation.
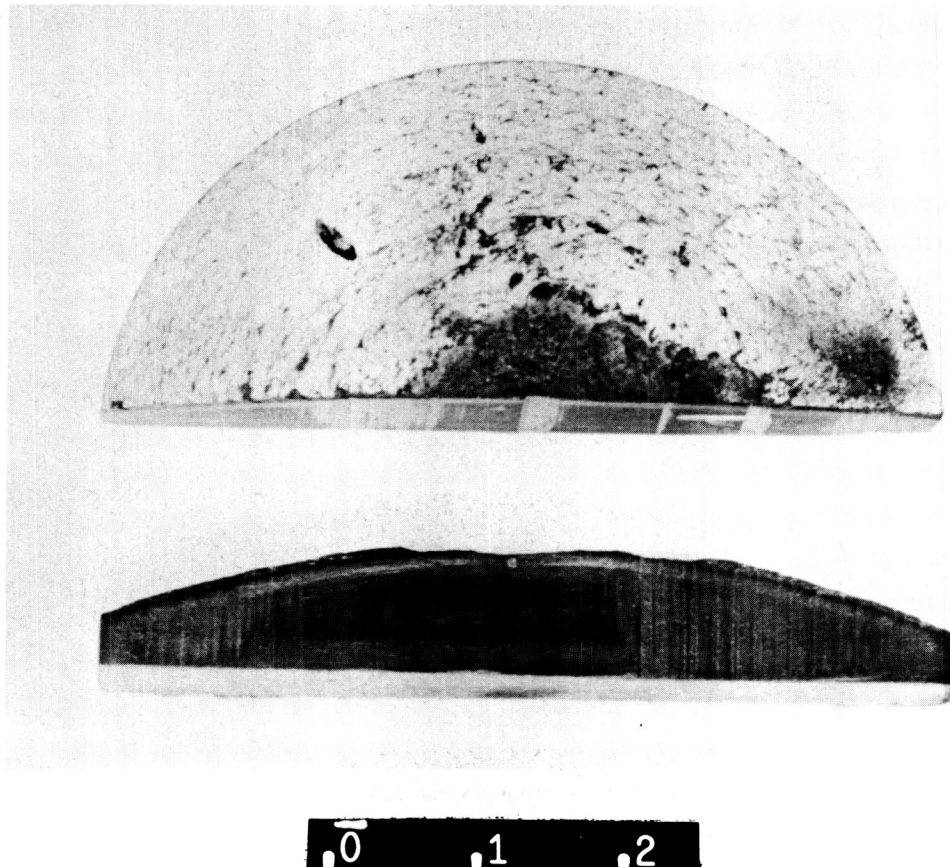
Stagnation temperature, $^{\circ}F$	3,300
Test time, sec	40.00
Weight loss, lb	0.160

Figure 12.- Surface appearance of Raybestos 42RPD specimen after ablation.
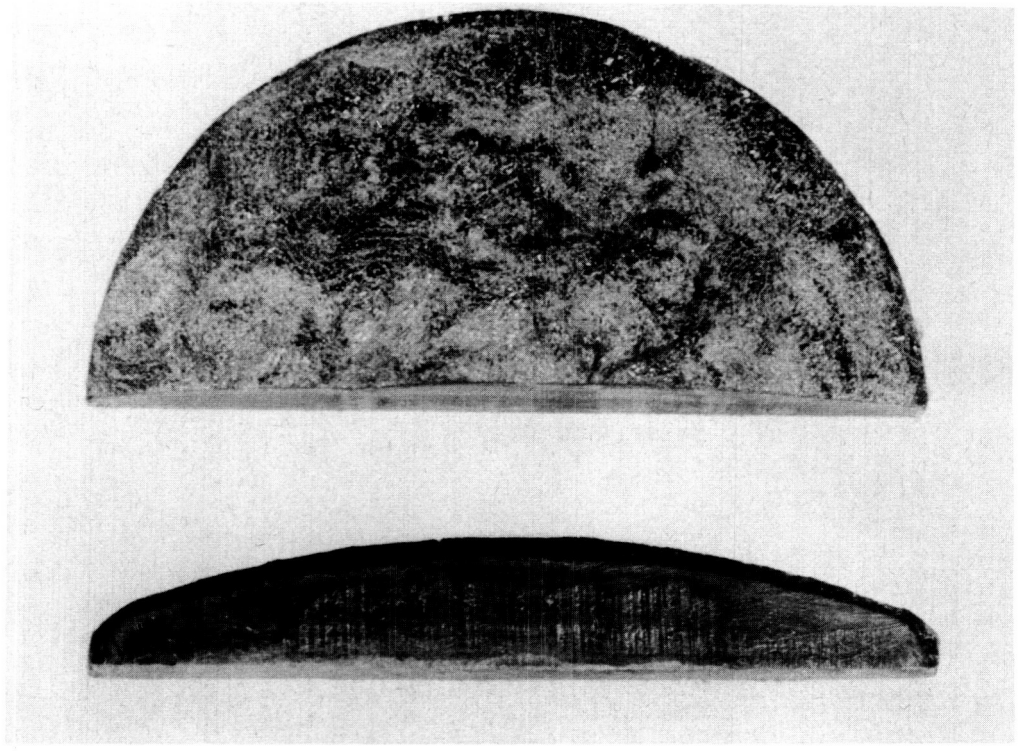
L-58-625a

Stagnation temperature, °F 3,300
Test time, sec 30.00
Weight loss, lb 0.230

Figure 13.- Surface appearance of Cincinnati Testing Laboratory speci-
men after ablation.
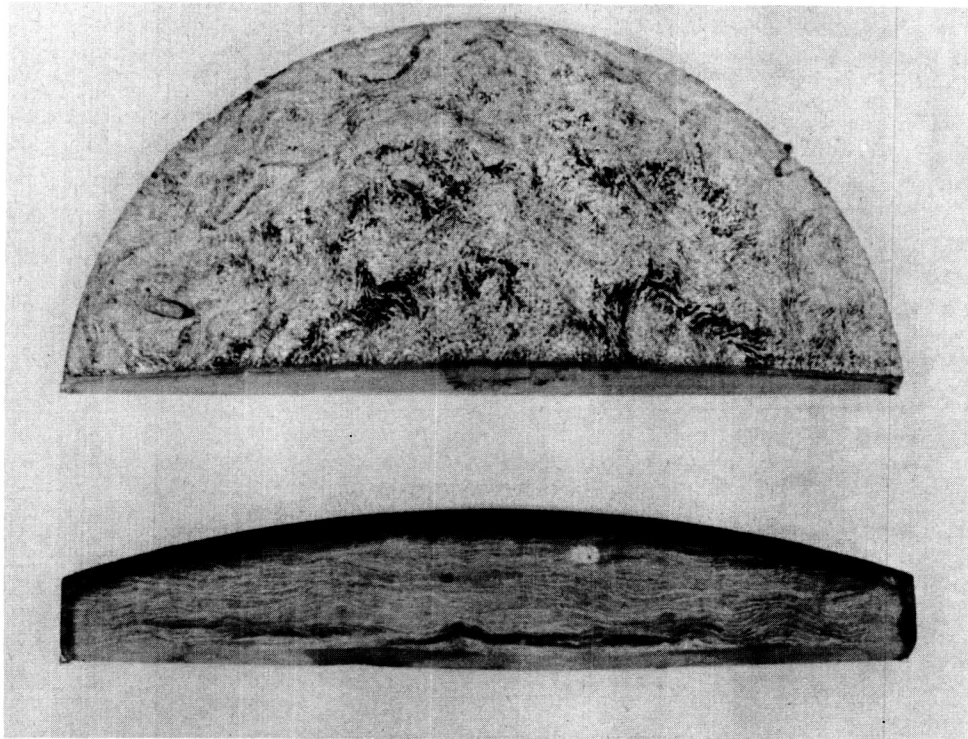
Stagnation temperature, °F   3,300
Test time, sec 20.00
Weight loss, lb 0.0588

Figure 14.- Surface appearance of Astrolite specimen after ablation.
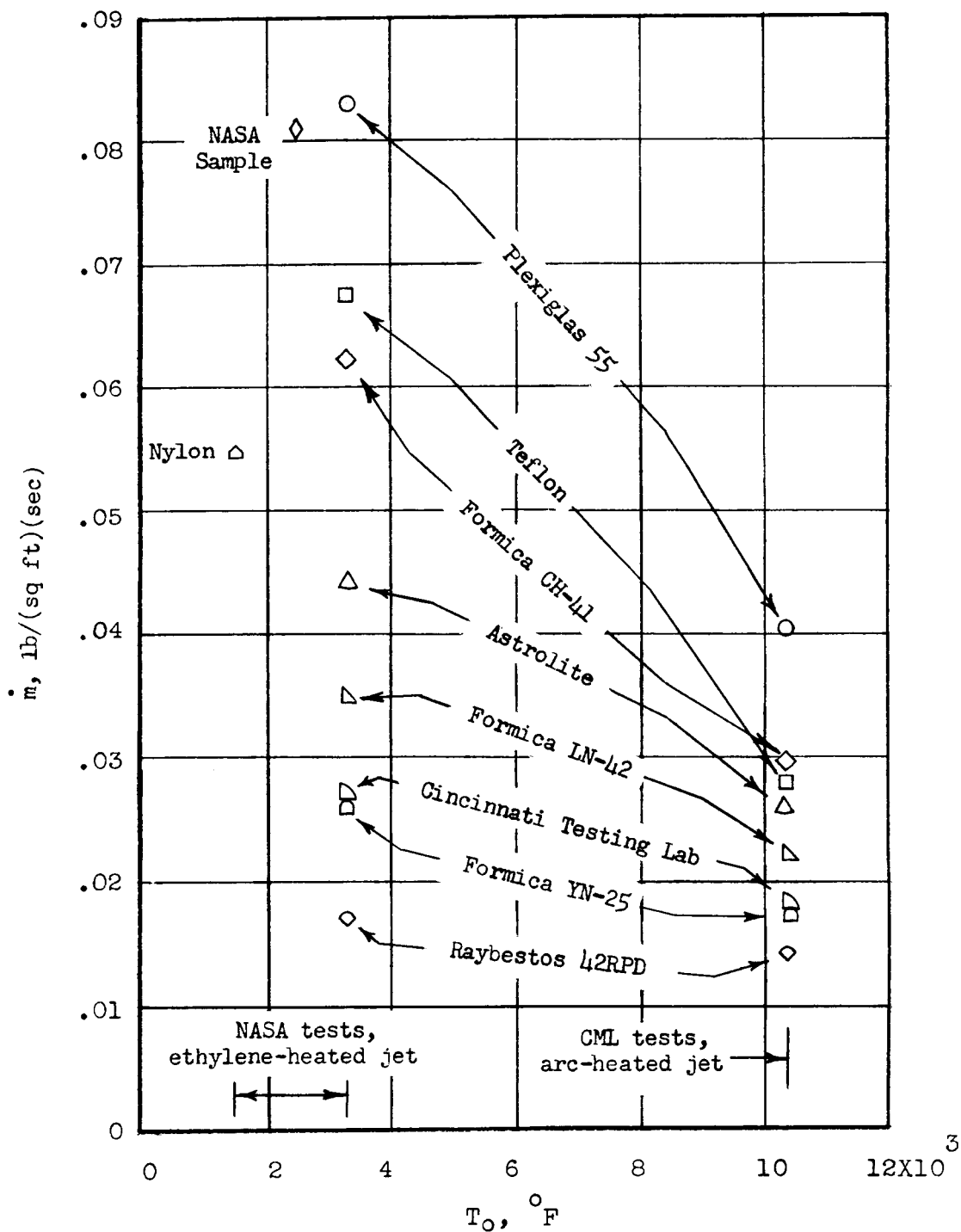
Figure 15.- Stagnation-point ablation rate as a function of the stagnation temperature.
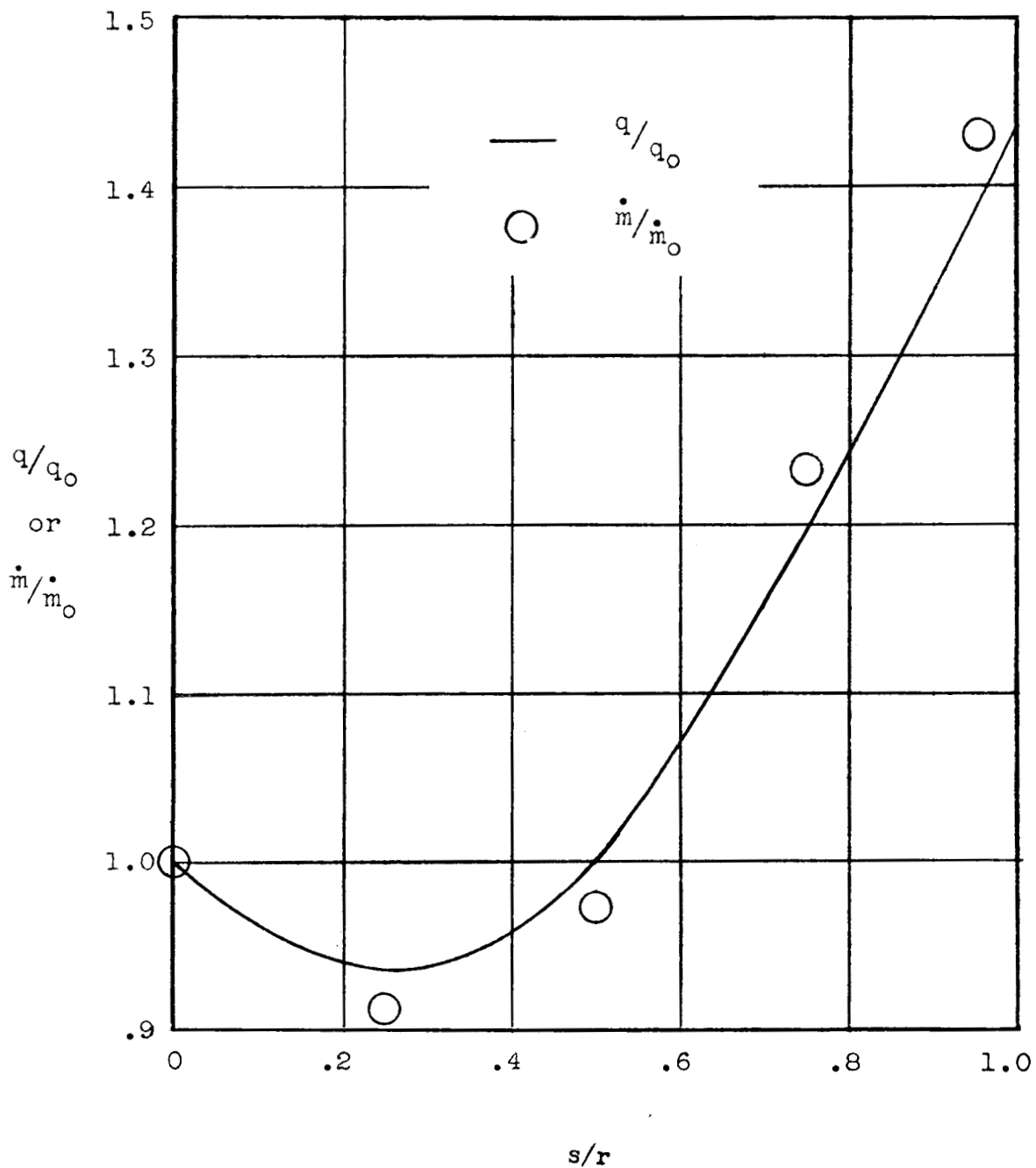
Figure 16.- Variation of the ablation rates and heat fluxes across the nose shape of the nylon model. $T_O = 1,750^O$ F; $\dot{m}_O = 0.05472$.
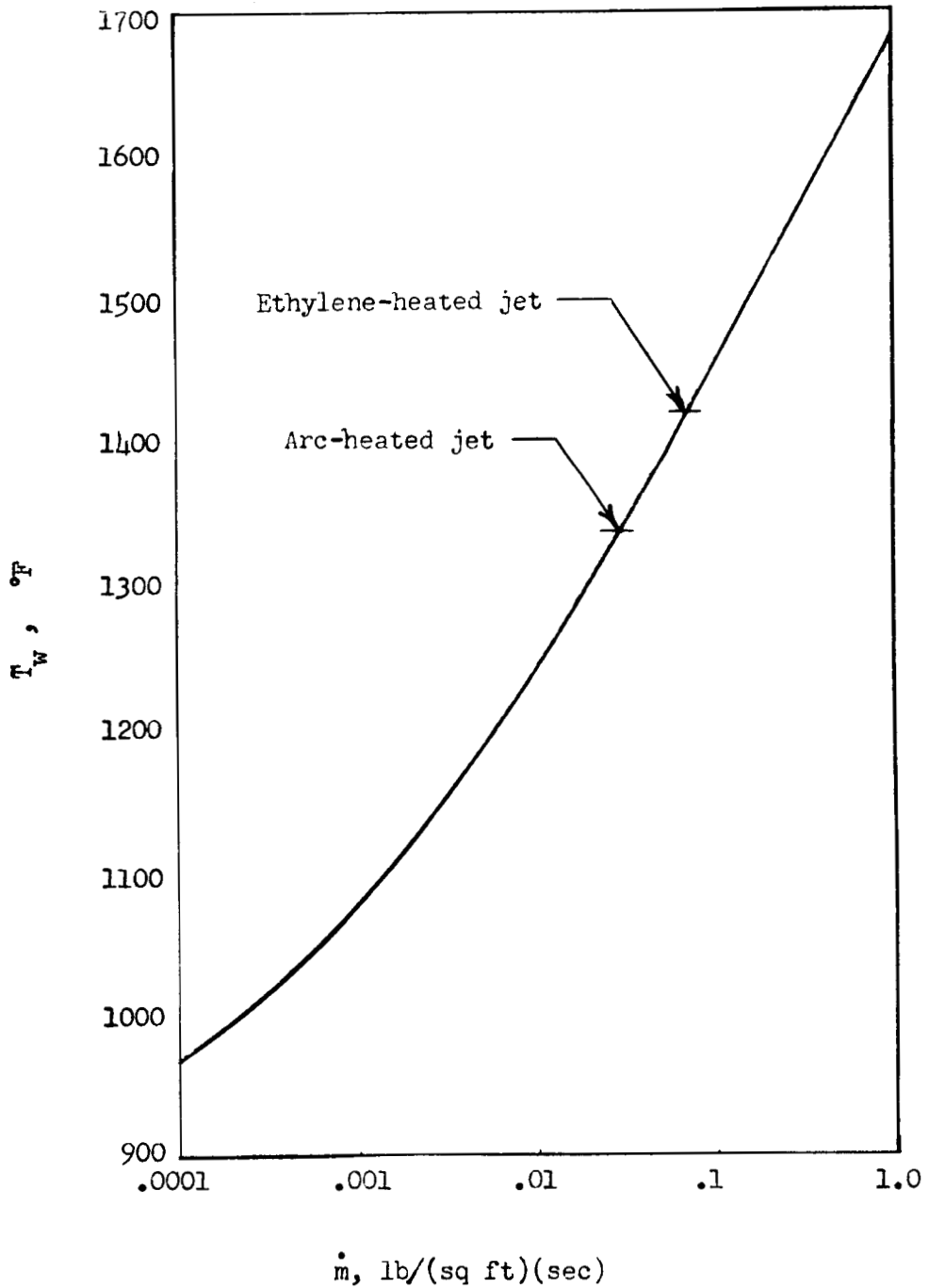
Figure 17.- Calculated variation of surface temperature with ablation rate for Teflon.
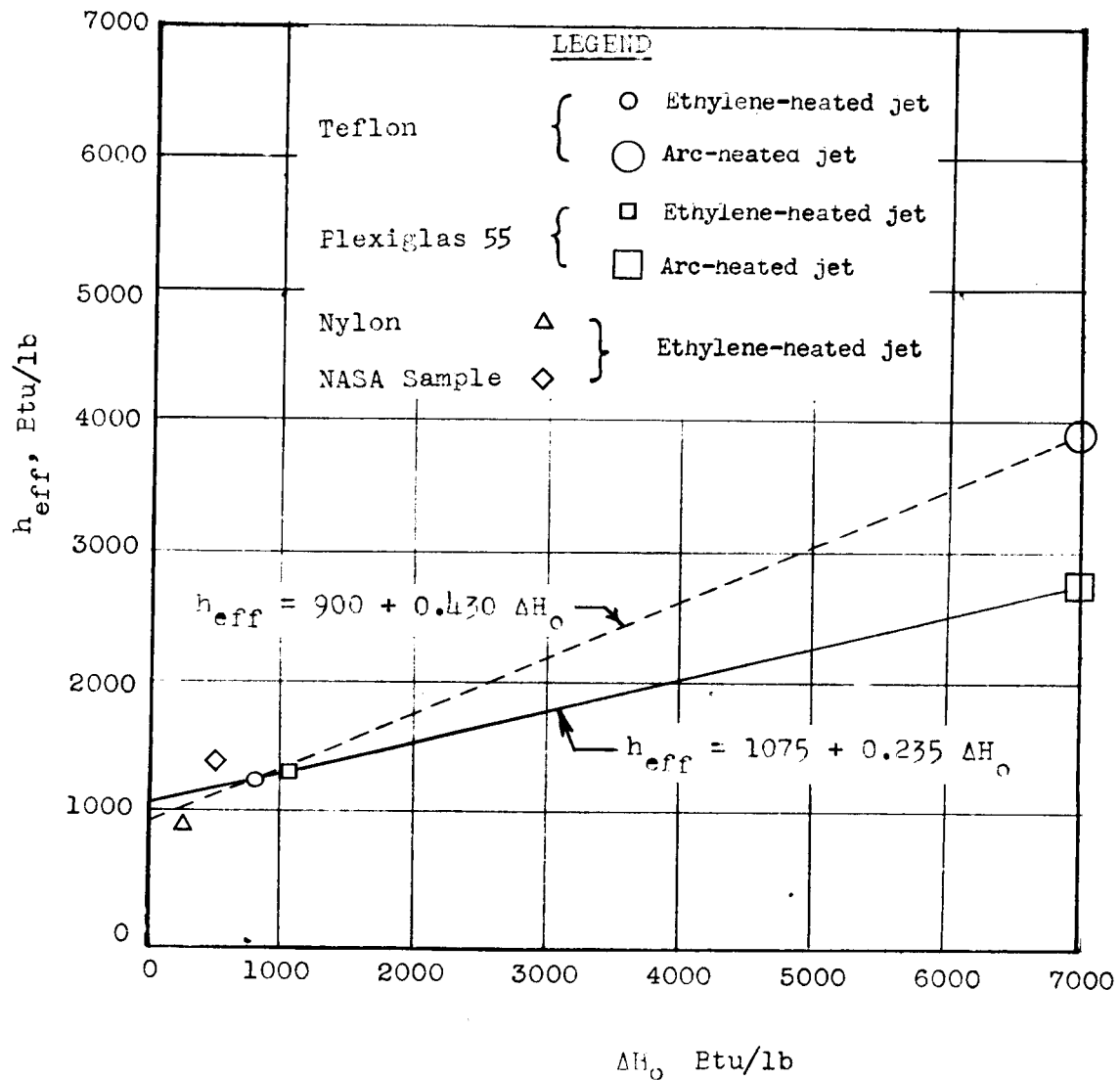
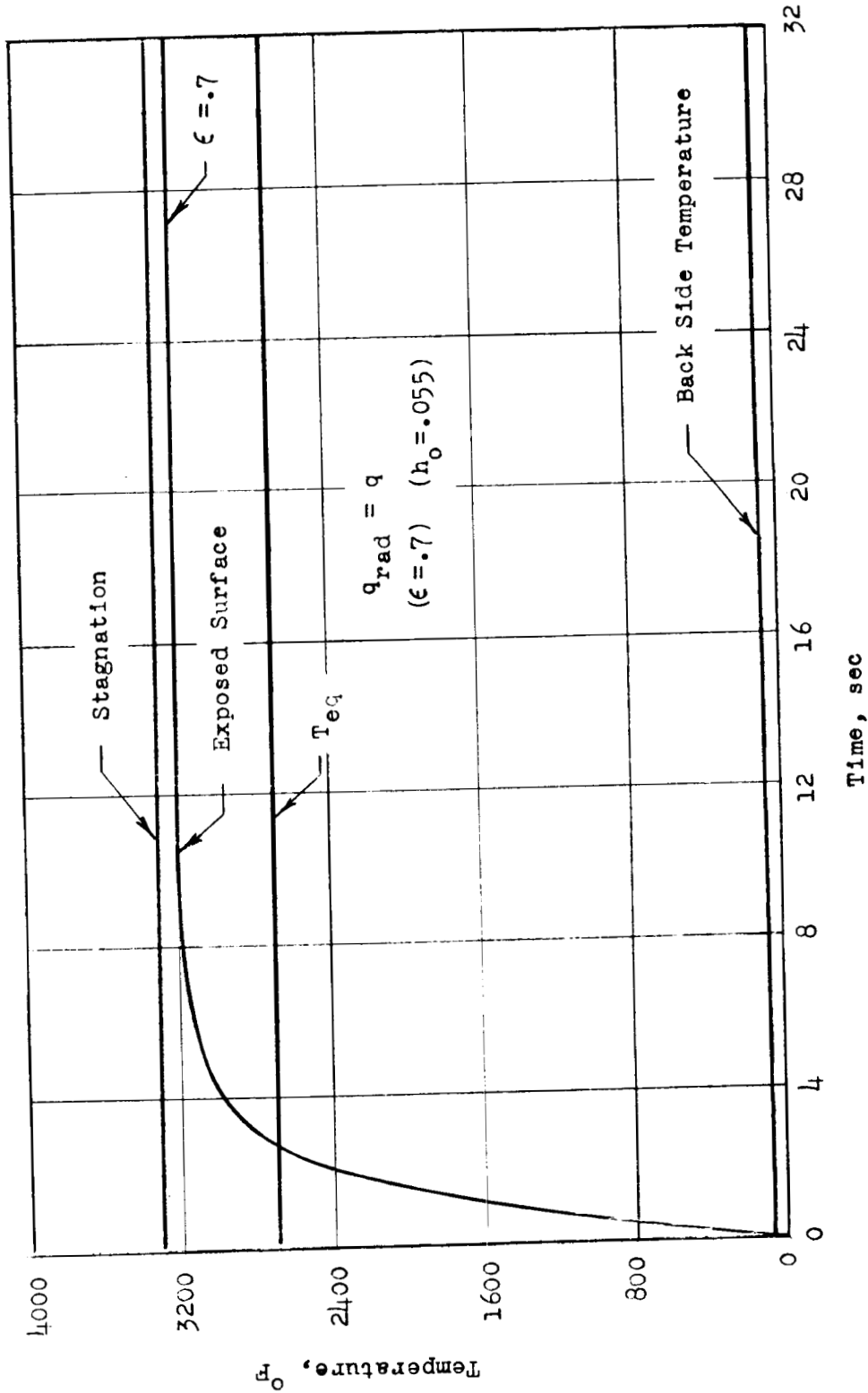Figure 18.- Effective heats of ablation as a function of the enthalpy potential.

Figure 19.- Temperature histories for the Formica YN-25 model. $T_O = 3,300^O$ F.
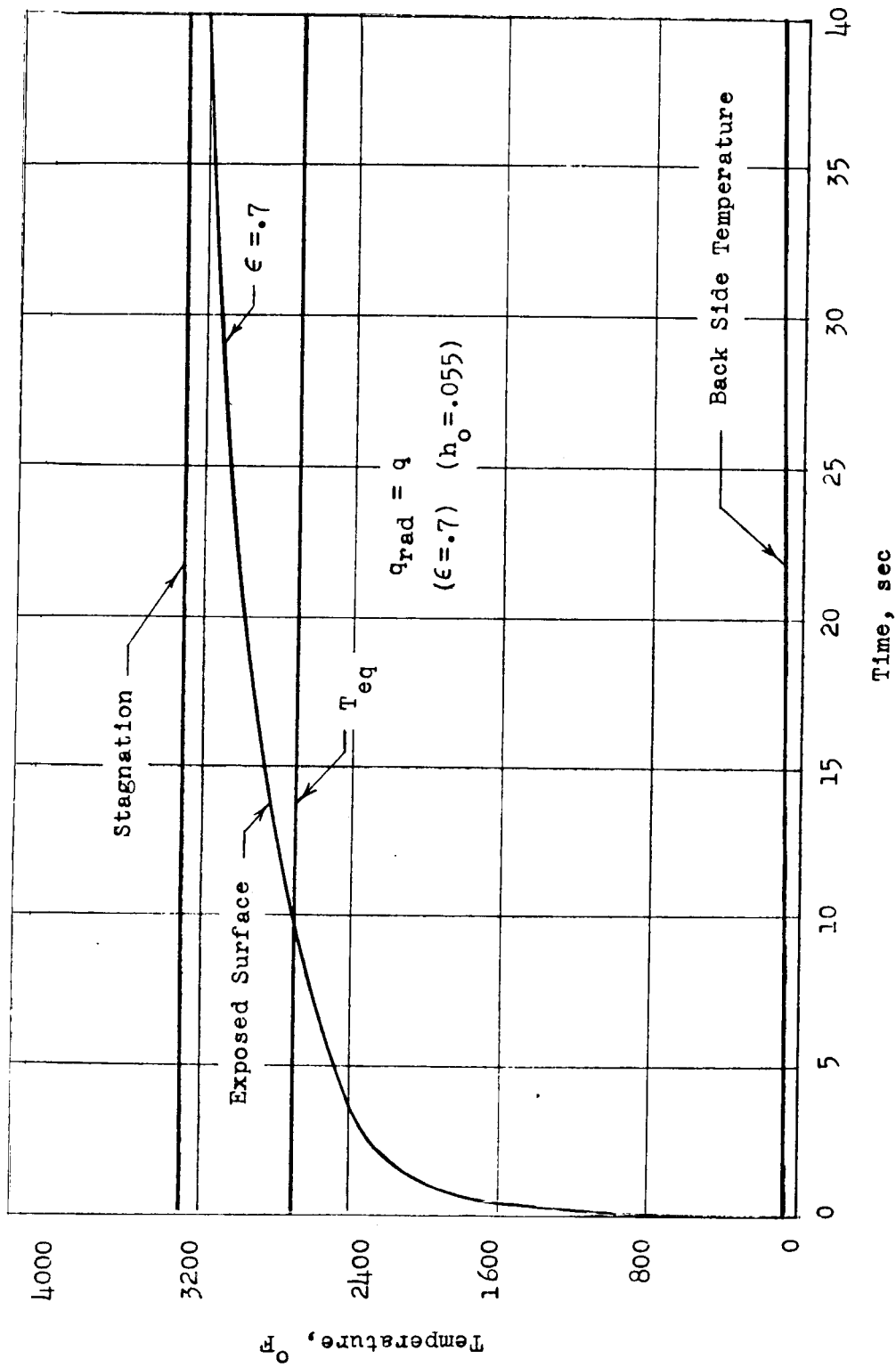
Figure 20.- Temperature histories for the Raybestos 42RPD model. $T_0 = 3,300°$ F.
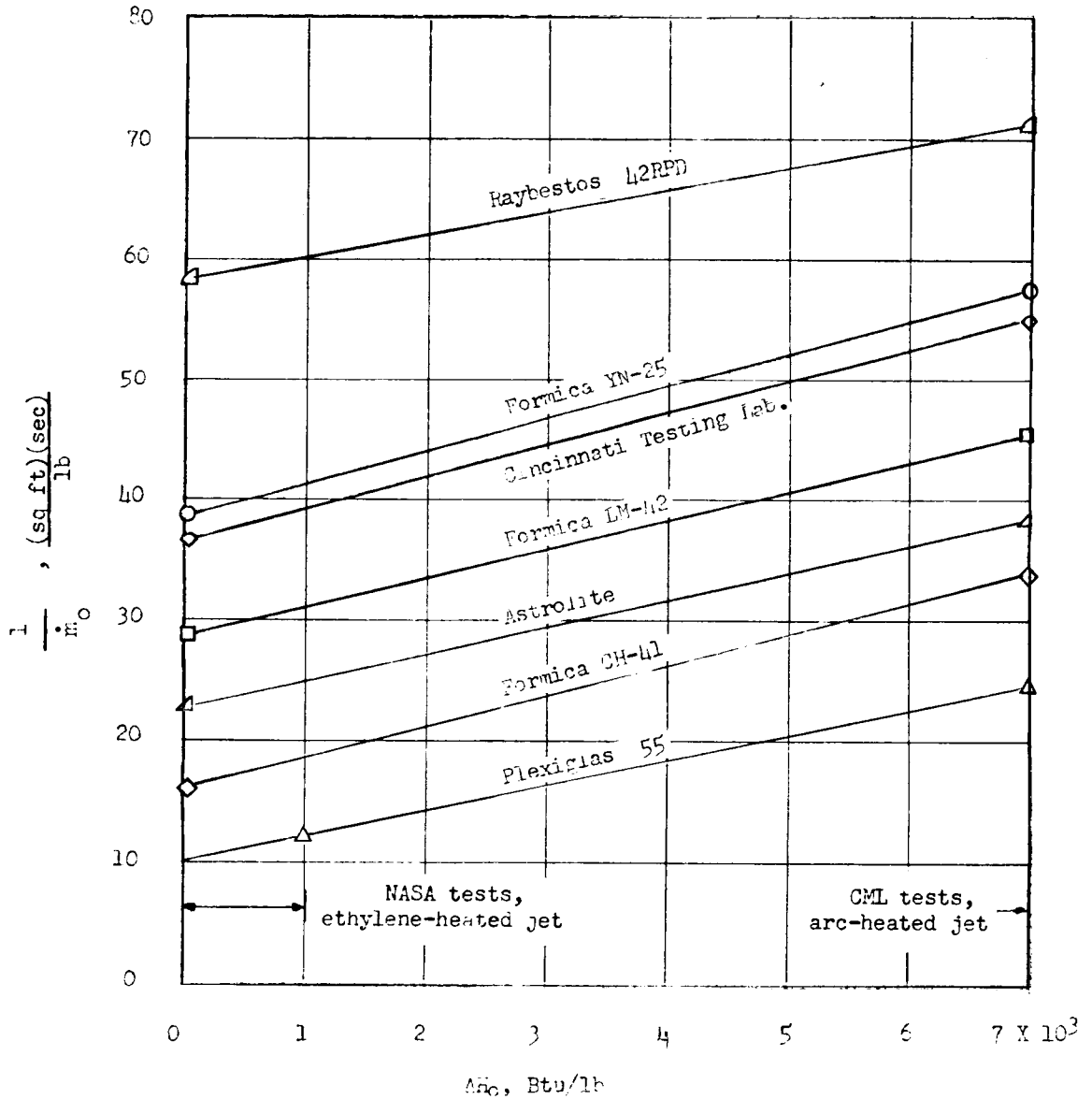
Figure 21.- Material effectiveness variation with enthalpy potential of the reinforced plastic materials.